

Where have all the interstellar silicon carbides gone?

Tao Chen^{1,2,5*}, C.Y. Xiao^{1,5†}, Aigen Li^{3‡}, and C.T. Zhou^{4§}

¹*Department of Astronomy, Beijing Normal University, Beijing 100875, China*

²*Department of Theoretical Chemistry and Biology, Royal Institute of Technology, 10691, Stockholm, Sweden*

³*Department of Physics and Astronomy, University of Missouri, Columbia, MO 65211, USA*

⁴*College of Engineering Physics, Shenzhen Technology University, Shenzhen 518118, China*

⁵*TC and CYX contributed equally.*

ABSTRACT

The detection of the $11.3\ \mu\text{m}$ emission feature characteristic of the Si–C stretch in carbon-rich evolved stars reveals that silicon carbide (SiC) dust grains are condensed in the outflows of carbon stars. SiC dust could be a significant constituent of interstellar dust since it is generally believed that carbon stars inject a considerable amount of dust into the interstellar medium (ISM). The presence of SiC dust in the ISM is also supported by the identification of presolar SiC grains of stellar origin in primitive meteorites. However, the $11.3\ \mu\text{m}$ absorption feature of SiC has never been seen in the ISM and oxidative destruction of SiC is often invoked. In this work we quantitatively explore the destruction of interstellar SiC dust through oxidation based on molecular dynamics simulations and density functional theory calculations. We find that the reaction of an oxygen atom with SiC molecules and clusters is exothermic and could cause CO-loss. Nevertheless, even if this is extrapolable to bulk SiC dust, the destruction rate of SiC dust through oxidation could still be considerably smaller than the (currently believed) injection rate from carbon stars. Therefore, the lack of the $11.3\ \mu\text{m}$ absorption feature of SiC dust in the ISM remains a mystery. A possible solution may lie in the currently believed stellar injection rate of SiC (which may have been overestimated) and/or the size of SiC dust (which may actually be considerably smaller than submicron in size).

Key words: stars: carbon; circumstellar matter; dust; stars: AGB and post-AGB; stars: mass-loss;

1 INTRODUCTION

Nearly nine decades ago, Wildt (1933) had already argued that solid silicon carbide (SiC) grains might form in N-type stars. It is now well recognized that SiC solids are a major dust species, second to amorphous carbon grains, condensed in the cool atmospheres of mass-losing, carbon-rich asymptotic giant branch (AGB) stars (e.g., see Nanni et al. 2021). This was originally computationally demonstrated over half a century ago by Friedemann (1969) and Gilman (1969) based on molecular equilibrium calculations, and observationally confirmed later by Treffers & Cohen (1974) who, by the first time, detected in two carbon stars, IRC+10216 and IRC+30219, a broad emission band in between 788 and $973\ \text{cm}^{-1}$ attributed to SiC dust. Subsequent spectroscopic

observations have revealed the widespread presence of SiC grains in carbon stars through the prominent $11.3\ \mu\text{m}$ emission feature characteristic of the Si–C stretch of SiC solids (Speck et al. 1997, Mutschke et al. 1999).¹ In addition, presolar SiC grains of stellar origin have also been identified in primitive meteorites based on isotope anomalies (e.g., see Bernatowicz et al. 1987).

Although the exact mass fraction of the condensates in carbon stars which are in the form of SiC is not precisely known and it depends on stellar mass and metallicity (Nanni et al. 2021), radiative transfer modeling of the observed infrared emission of carbon stars has shown that the

¹ In principle, essentially all carbon star should make SiC. Observationally, SiC dust is harder to detect in redder stars as the contrast with amorphous carbon becomes smaller. The $11.3\ \mu\text{m}$ SiC feature strength with respect to the dust thermal emission continuum has been seen to increase with the stellar metallicity and show a trend with the stellar mass-loss rate (e.g., see Sloan et al. 2016, Kramer et al. 2019, Nanni et al. 2021).

* taochen@kth.se

† xiaocunying@bnu.edu.cn

‡ lia@missouri.edu

§ zcangtao@sztu.edu.cn

mass ratio of SiC to amorphous carbon could be as much as $\sim 25\%$ for the Milky Way (e.g., see Groenewegen et al. 1998) and $\sim 43\%$ for the Large Magellanic Cloud and $\sim 11\%$ for the Small Magellanic Cloud (Groenewegen et al. 2009, Nanni et al. 2019). Theoretical dust-yield calculations have predicted that the mass fraction of SiC over the total dust (i.e., SiC plus amorphous carbon) produced in carbon stars of an initial mass of $3 M_{\odot}$ around solar metallicity is $\sim 25\%$ (Nanni et al. 2013; also see Zhukovska & Henning 2013), although different AGB models produce different yields at varying metallicity because of the uncertainties in modelling the mass-loss and third-dredge up processes (e.g., see Nanni et al. 2013, 2014, 2019; Ventura et al. 2012, 2014, 2018).

Solid grains—SiC and amorphous carbon condensed in carbon stars as well as silicates and oxides condensed in oxygen-rich stars will be driven out of the stellar atmospheres and injected into the interstellar medium (ISM) by radiation pressure. If the contribution of carbon stars to the Galactic dust budget is about comparable to that of oxygen-rich stars as generally believed (e.g., see Gehrz 1989), then SiC should be a significant constituent of interstellar dust. However, the nondetection of the characteristic $11.3 \mu\text{m}$ feature of SiC in the ISM puts this at odds (Whittet et al. 1990). In this work we explore the physical and chemical processes subjected by SiC in the ISM, with special attention paid to the destruction of SiC by oxidation. We apply the Born-Oppenheimer molecular dynamics (BOMD; Helgaker et al. 1990, Uggerud & Helgaker 1992) and density functional theory (DFT; Lee et al. 1988, Becke 1992) to investigate the oxidation reaction pathway related to SiC grains in the ISM. The DFT technique is among the most popular and versatile methods for computational quantum-mechanical modelling of molecules and clusters. In comparison with other quantum chemical methods, DFT simplifies the N -body problem to a tractable $3N$ non-interacting system, which makes DFT more efficient and scalable for large systems. In BOMD simulations, the energies and forces are computed from DFT at quantum levels. Therefore, the BOMD method is more accurate than classical molecular dynamics in which the energies and forces are calculated from empirical formulae or force fields.

2 COMPUTATIONAL METHODS

A typical, submicron-sized SiC grain contains hundreds of millions of atoms (e.g., there are $\sim 4 \times 10^8$ atoms in a spherical SiC grain of radius $a = 0.1 \mu\text{m}$). Even for SiC nanoparticles, it is extremely expensive to study such systems with *ab initio* methods like BOMD and DFT, requiring tremendous computational power and time. Nevertheless, it is generally believed that SiC grains are built up via bottom-up processes, starting with small gas-phase molecules and successive growth to clusters by molecular additions. Thus, SiC clusters are indispensable for the formation of SiC grains – they are the initial states of SiC grains (e.g., see Gobrecht et al. 2017). Therefore, SiC molecules and clusters could be reasonable candidates or alternatives of SiC grains for molecular dynamics modeling. To this end, we consider the

most favourable structures of Si_3C_3 and $\text{Si}_{12}\text{C}_{12}$,² with the former representing a triangle structure (see Figure 4a of Gobrecht et al. 2017, also see Mülh user et al. 1993) with a high surface-to-volume ratio and the latter exhibiting a spherical structure (see Figure 16a of Gobrecht et al. 2017, also see Watkins et al. 2009) and possessing a low surface-to-volume ratio. Si_3C_3 is selected because it is the smallest cluster with a 3D structure (see Gobrecht et al. 2017) and thus allows us to investigate the reactions for the low-end cluster. $\text{Si}_{12}\text{C}_{12}$ is selected because of its bucky-like symmetrical structure which minimizes the considerations of the incident directions of oxygen atoms. $\text{Si}_{16}\text{C}_{16}$ is also symmetrical in structure but it is computationally more expensive (see Gobrecht et al. 2017).

To evaluate the stability or reactivity of the studied molecule or cluster, we calculate the binding and dissociation energies and transition barriers for each target system, using DFT as implemented in the Gaussian16 package (Frisch et al. 2016). All structures are optimized to their ground states using the 6-311++G(2d,p) basis set. Here the Slater-type atomic orbitals (AOs) are described by “basis functions” and each basis function is described by a sum of several Gaussian functions. To take the intermolecular forces into account, the D3 version of Grimme’s dispersion with Becke-Johnson damping (Grimme et al. 2011) is included in the calculations. Here, “D3” denotes a function of interatomic distances, which contains adjustable parameters that are fitted to the conformational and interaction energies computed using high-level methods.

The vibrational frequencies are calculated under the harmonic oscillator approximation for the optimized geometries. The transition states are estimated based on our molecular dynamics simulations followed by relaxed scanning (with geometry optimization at each point) on the potential energy surface (PES). The transition barrier is calculated as the energy difference between the ground states of the reactant and the transition state. For reactions without transition state, the dissociation energy is computed as the energy difference between the ground states of the reactant and the product. The intermolecular forces are taken into account in all the calculations. The dynamical processes are simulated using BOMD (Helgaker et al. 1990, Uggerud & Helgaker 1992) as implemented in the Gaussian16 package (Frisch et al. 2016). The B3LYP hybrid functional in combination with the 6-31G(d,p) basis set is utilized for the BOMD simulations. For all these simulations, again, the D3 version of Grimme’s dispersion with Becke-Johnson damping (Grimme et al. 2011) is also included.

3 RESULTS

Over 30 years ago, Whittet et al. (1990) searched for the $11.3 \mu\text{m}$ absorption band of SiC in the diffuse ISM along the line of sight toward the Galactic center. The lack of any spectral evidence for solid SiC led Whittet et al. (1990) to place an upper limit on the abundance of silicon relative to hydrogen (i.e., Si/H) in SiC dust to be at most $\sim 5\%$ of that

² Si_3C_3 has many isomers and the number of structural isomers for $\text{Si}_{12}\text{C}_{12}$ gets literally astronomical. Here we are confined to the isomers with the lowest energy.

in silicate dust. They speculated that SiC grains could be destroyed in the ISM by oxidation. Motivated by this, we first model the interaction between a Si_3C_3 molecule and an incident oxygen atom. This applies to the diffuse ISM where atomic oxygen is the dominant form of gaseous oxygen. The oxidation of SiC solids by O_2 has been extensively studied experimentally (e.g., see Ervin 1958) and is not relevant since there is little O_2 in the ISM (e.g., see Larsson et al. 2007). In dense molecular clouds where oxygen is mostly locked up in water ice, SiC dust, if present, is expected to be coated by a layer of water ice and oxidation is unlikely since the reaction of SiC with water to produce SiO_2 and methane only takes place at a temperature of above 1300°C (e.g., see Park et al. 2014).

As the oxygen atom is much smaller than a SiC cluster or grain, the incident oxygen atom would only influence a few atoms in the target SiC cluster or grain, i.e., the reaction would only take place in an area near the incident atom and depends on the incident direction. Figure 1 shows the BOMD simulations for collisions between a Si_3C_3 molecule and an incident oxygen atom arriving from three different directions. The simulations demonstrate that, due to the impact of an oxygen atom, CO and SiO molecules can be released rapidly from the molecule within 1 ps. The fragmentation products are highly dependent on the incoming direction of the oxygen atom: if the oxygen atom first collides with a carbon atom, then a CO molecule is formed and ejected, while a SiO-loss would be triggered if the incident oxygen atom first hits a silicon atom.

To better understand the reaction mechanism, DFT calculations for the three reaction scenarios as illustrated in Figure 1 are performed and shown in Figure 2. The corresponding binding energies for $\text{O} + \text{Si}_3\text{C}_3$ and dissociation energies for $\text{Si}_3\text{C}_3\text{O} - \text{CO}$ or $\text{Si}_3\text{C}_3\text{O} - \text{SiO}$ are illustrated in Figure 2 as well. Most prominently, the reactions for absorbing an oxygen atom to a Si_3C_3 molecule are *exothermic*, which release $\sim 7\text{--}9\text{ eV}$ energy, depending on the incoming direction of the incident oxygen atom. This is not surprising since association reactions of the form $\text{A} + \text{B} \rightarrow \text{AB}$ are usually exothermic, as the number of bonds is increased in the product. The energy generated from these reactions will traverse through all of the vibrational modes of the molecule, and the chemical bonds with lower binding energies will be dissociated. Moreover, for the $\text{Si}_3\text{C}_3\text{O}$ system SiO-loss is also an exothermic reaction, which releases $\sim 1\text{ eV}$ energy. In contrast, CO has a binding energy of $\sim 0.6\text{ eV}$ and therefore it requires $\sim 0.6\text{ eV}$ to eject CO from the $\text{Si}_3\text{C}_3\text{O}$ system. However, with the much larger amount of energy ($\sim 7\text{--}9\text{ eV}$) gained from the first step, such a low binding energy can be easily crossed, leading to a rapid CO-loss.

The collisions between an oxygen atom with larger molecules, e.g., $\text{Si}_{12}\text{C}_{12}$, demonstrate a rather different scenario. Figure 3 shows the BOMD simulations for collisions between an oxygen atom and a $\text{Si}_{12}\text{C}_{12}$ molecule. No fragmentation is found, instead, the oxygen atom is captured by the $\text{Si}_{12}\text{C}_{12}$ molecule. The symmetry of the molecule is broken due to the incoming oxygen atom, which forms two new covalent bonds, one connected with a carbon atom and the other one connected with a silicon atom. The DFT calculations show that, as illustrated in Figure 4, the absorption of an oxygen atom is still an exothermic reaction, which releases $\sim 7.5\text{ eV}$ energy. However, the dissociation of CO

and SiO requires $\sim 2.6\text{ eV}$ and $\sim 4.0\text{ eV}$, respectively. Due to its larger size, $\text{Si}_{12}\text{C}_{12}$ could redistribute the excess energy across its degrees of freedom to avoid fragmentation.

Nevertheless, in the diffuse ISM oxygen atoms are far more abundant than SiC grains.³ It is therefore highly probable that a SiC grain would be hit by multiple oxygen atoms. Figure 5 shows the collisions of $\text{Si}_{12}\text{C}_{12}\text{O}$ with another oxygen atom. The $\text{Si}_{12}\text{C}_{12}\text{O}$ molecule is adopted from the simulation illustrated in Figure 3 but is set to its vibrationally ground state. Two opposite incident directions are simulated for the incoming oxygen atom. In both cases, we see CO loss within 1 ps. This is because, the presence of oxygen atoms (aka O-substituted molecules) decreases the transition energy barriers in the region where the oxygen atom is located, which makes CO-losses highly favorable in comparison to other channels.

4 DISCUSSION

We have shown in §3 that the reaction between an oxygen atom and a SiC molecule is exothermic and would result in CO-loss almost instantly for small SiC molecules, or after the absorption of one or several oxygen atoms for large SiC molecules. Therefore, the destruction rate of SiC in the ISM is essentially determined by the collision rate of oxygen atoms with SiC grains. Let n_{O} be the number density of oxygen atoms in the diffuse ISM, v_{O} be the mean thermal velocity of oxygen atoms, and τ_{coll} be the collision time scale of an oxygen atom with a SiC grain of radius a . The collision rate (in s^{-1}) is $\tau_{\text{coll}}^{-1} = n_{\text{O}} v_{\text{O}} \pi a^2$, where $n_{\text{O}} \approx [\text{O}/\text{H}]_{\text{gas}} n_{\text{H}}$, $v_{\text{O}} = \sqrt{3k_{\text{B}}T_{\text{gas}}/m_{\text{O}}}$, n_{H} is the hydrogen number density, k_{B} is the Boltzman constant, T_{gas} is the gas temperature, and m_{O} is the mass of an oxygen atom. If we adopt an interstellar gas-phase oxygen abundance of $[\text{O}/\text{H}]_{\text{gas}} = 320\text{ ppm}$ (Meyer et al. 1998), $n_{\text{H}} = 1\text{ cm}^{-3}$ and $T_{\text{gas}} = 100\text{ K}$ for the diffuse ISM, we obtain $\tau_{\text{coll}} \approx 2.52 \times 10^8 \times (0.1\text{ }\mu\text{m}/a)^2\text{ s} \approx 7.99 \times (0.1\text{ }\mu\text{m}/a)^2\text{ yr}$.

Let $[\text{Si}/\text{H}]_{\text{SiC}}$ be the abundance of silicon (relative to hydrogen) tied up in SiC dust in the ISM, $\mu_{\text{SiC}} = 40$ be the molecular weight of SiC, $\rho_{\text{SiC}} \approx 3.2\text{ g cm}^{-3}$ be the mass density of SiC dust,⁴ $m_{\text{SiC}} = (4/3)\pi a^3 \rho_{\text{SiC}}$ be the mass of a spherical SiC grain of radius a , and M_{H} be the total interstellar hydrogen gas mass in the Milky Way. The total number of SiC grains would be $N_{\text{SiC}} \approx M_{\text{H}} [\text{Si}/\text{H}]_{\text{SiC}} \mu_{\text{SiC}} / m_{\text{SiC}} \lesssim 1.44 \times 10^{53} (0.1\text{ }\mu\text{m}/a)^3$, if we adopt $M_{\text{H}} = 4.9 \times 10^9 M_{\odot}$ (Draine 2011), $[\text{Si}/\text{H}]_{\text{SiC}} \lesssim 5\text{ ppm}$ (Whittet et al. 1990), and assume that all SiC grains have the same size a . If each collision of an oxygen atom with a SiC grain results in an ejection of CO, we would expect a total SiC dust mass

³ If we take a gas-phase abundance of $[\text{O}/\text{H}]_{\text{gas}} = 320\text{ ppm}$ for atomic oxygen in the diffuse ISM (Meyer et al. 1998), and assume that all SiC grains have the same size of $a = 0.1\text{ }\mu\text{m}$ and consume an upper limit of 5 ppm of Si/H (Whittet et al. 1990), the number density of oxygen atoms exceeds that of SiC grains by a factor of $\sim 1.3 \times 10^{10}$.

⁴ We note that such a mass density is applicable for bulk, macroscopic SiC dust. For small SiC clusters, this would underestimate the actual “size” since small SiC clusters are hollow and not compactly packed (e.g., such a mass density would imply a radius of $a \approx 3.90\text{ \AA}$ for a spherical $\text{Si}_{12}\text{C}_{12}$ cluster).

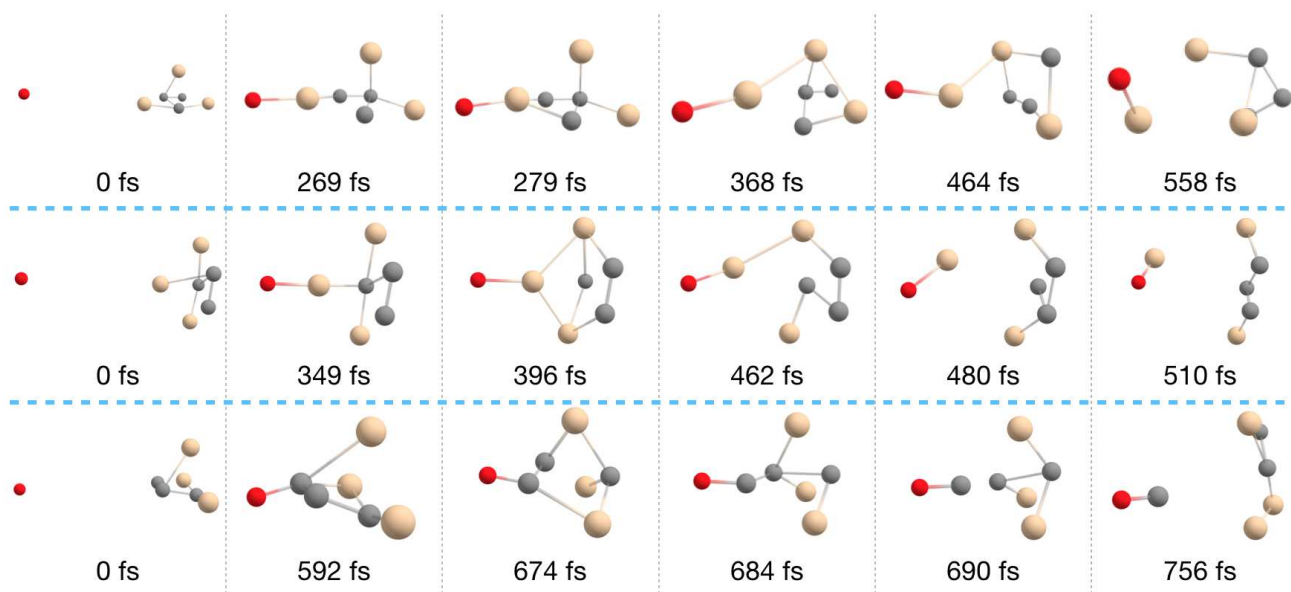


Figure 1. Snapshots from molecular dynamics simulations for collisions between an oxygen atom (red ball) and a Si_3C_3 molecule (in which gray balls represent carbon atoms and yellow balls correspond to silicon atoms), with the oxygen atom arriving from three different directions. The actual time in the simulation is shown beneath each molecular structure. SiO-loss (upper and middle panels) and CO-loss (bottom panel) can be seen on the rightmost panels.

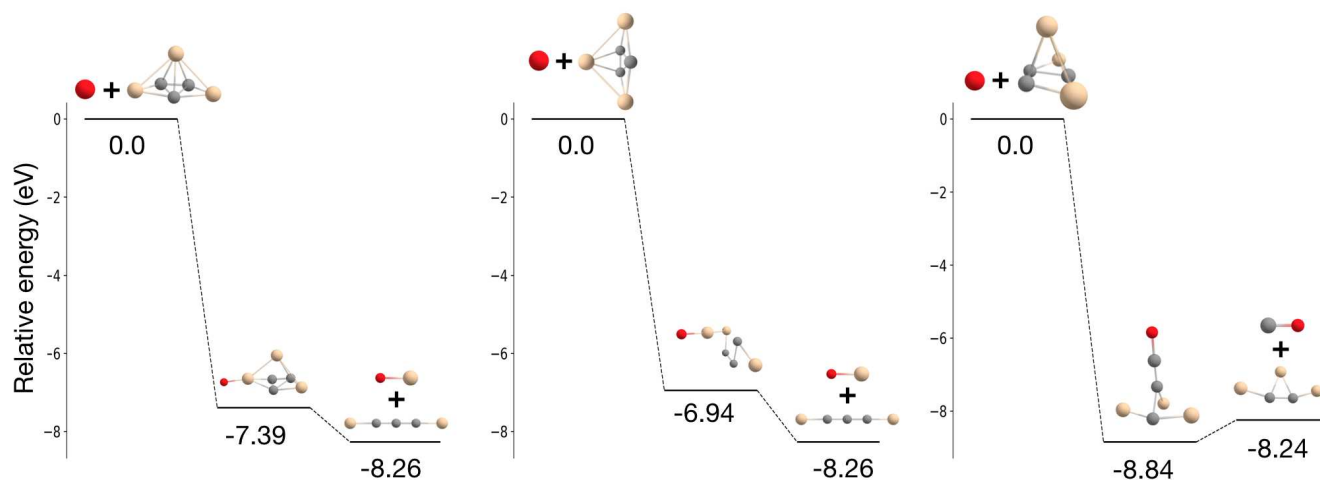


Figure 2. Calculated binding and dissociation energies for reactions between a Si_3C_3 molecule and an incident oxygen atom arriving at three different positions.

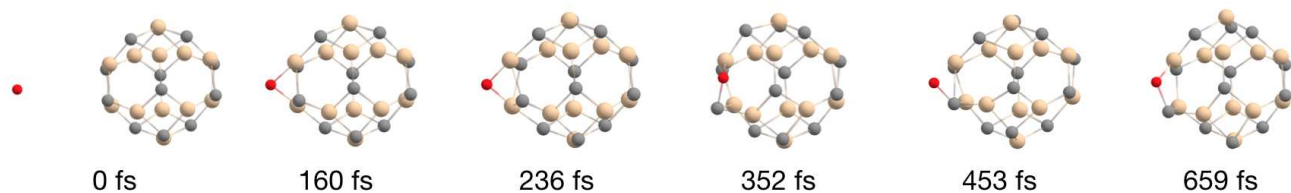


Figure 3. Snapshots from molecular dynamics simulations for collisions between an oxygen atom (red ball) and a $\text{Si}_{12}\text{C}_{12}$ molecule. Due to the high symmetry of $\text{Si}_{12}\text{C}_{12}$, only one incident direction is simulated for the oxygen atom.

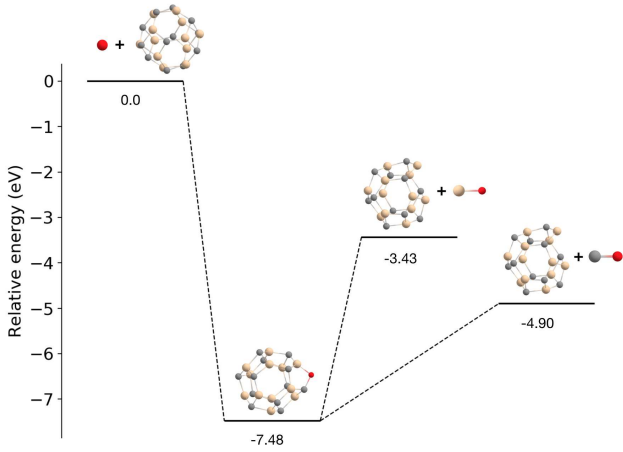


Figure 4. Calculated binding and dissociation energies for reactions between a $\text{Si}_{12}\text{C}_{12}$ molecule and an incident oxygen atom.

destruction rate of $(dM/dt)_{\text{SiC}}^{\text{des}} \approx 12m_{\text{H}}N_{\text{SiC}}/\tau_{\text{coll}} \lesssim 1.80 \times 10^{-4} (0.1 \mu\text{m}/a) M_{\odot} \text{yr}^{-1}$.

The injection rate of carbon dust from all carbon-rich objects including C, R, N, and S stars into the ISM was estimated to be $(dM/dt)_{\text{C}}^{\text{pro}} \approx 0.003 - 0.01 M_{\odot} \text{yr}^{-1}$ (Gehrz 1989). Let's assume the SiC dust injection rate from evolved stars to be 10% of that of carbon dust (see Groenewegen et al. 1998, 2009; Nanni et al. 2013, 2019). We would then expect that each year carbon stars eject about $(3 - 10) \times 10^{-4} M_{\odot}$ of SiC dust into the ISM, i.e., $(dM/dt)_{\text{SiC}}^{\text{pro}} \approx 10\% \times (dM/dt)_{\text{C}}^{\text{pro}} \approx (3 - 10) \times 10^{-4} M_{\odot} \text{yr}^{-1}$. Compared with the SiC destruction rate of $(dM/dt)_{\text{SiC}}^{\text{des}} \lesssim 1.80 \times 10^{-4} (0.1 \mu\text{m}/a) M_{\odot} \text{yr}^{-1}$, it is clear that one requires the interstellar SiC grains to be smaller than $\sim 0.02 \mu\text{m}$ (for $(dM/dt)_{\text{SiC}}^{\text{pro}} = 3 \times 10^{-4} M_{\odot} \text{yr}^{-1}$) or $\sim 0.06 \mu\text{m}$ (for $(dM/dt)_{\text{SiC}}^{\text{pro}} = 1 \times 10^{-3} M_{\odot} \text{yr}^{-1}$) in order for the destruction rate to exceed the current injection rate from carbon stars, i.e., $(dM/dt)_{\text{SiC}}^{\text{des}} \gtrsim (dM/dt)_{\text{SiC}}^{\text{pro}}$. However, presolar SiC grains of stellar origin identified in primitive meteorites are mostly submicron-sized.⁵

As we have already generously assumed that one collision leads to the ejection of one CO molecule despite that for large SiC molecules multiple collisions are needed, we conclude that the destruction rate of SiC dust by oxidation is unlikely larger than the stellar injection rate and therefore the nondetection of the $11.3 \mu\text{m}$ absorption feature of SiC dust in the diffuse ISM cannot be explained by the destruction of SiC dust through oxidation. It is true that the kinetic reactions of oxygen atoms with bulk, macroscopic SiC dust certainly differ from that of oxygen atoms with molecular SiC clusters. However, the destruction rates of SiC dust derived above do not rely on the exact oxidation rates of SiC clusters. Indeed, the only assumption made in deriving

$(dM/dt)_{\text{SiC}}^{\text{des}}$ is that we have assumed that each collision of an oxygen atom with a SiC dust grain would result in an ejection of CO. As mentioned above, this would result in an overestimation of $(dM/dt)_{\text{SiC}}^{\text{des}}$ since for large SiC clusters a single collision is unlikely capable of releasing CO.

While the $11.3 \mu\text{m}$ absorption feature could be suppressed in large SiC grains of $a > 1 \mu\text{m}$, presolar SiC grains as mentioned earlier, have indicated the predominant presence of submicron-sized SiC grains. Perhaps submicron-sized SiC grains only constitute a small fraction of the SiC dust condensed in carbon stars and then ejected into the ISM. Cristallo et al. (2020) examined the evolution of the AGB stars that polluted the solar system at 4.57 Gyr ago and found that the submicron-sized presolar SiC grains predominantly originated from AGB stars with solar metallicity and an initial mass of $\sim 2 M_{\odot}$. Theoretical calculations have shown that the typical grain size of SiC condensed in AGB stars can be dependent on the stellar metallicity and can be smaller than presolar SiC grains for stars with metallicities lower than solar (e.g., see Figures 11 and 12 in Nanni et al. 2013, Sect. 5.3 in Ventura et al. 2014, Section 5.3). If the majority of the interstellar SiC grains originated from AGB stars are smaller than $0.02 \mu\text{m}$ or even nano-sized, they will be destroyed more rapidly than the currently believed stellar injection rate since the SiC destruction rate increases as the SiC dust size decreases, $(dM/dt)_{\text{SiC}}^{\text{des}} \propto 1/a$. In the diffuse ISM, nano-sized SiC grains will be stochastically heated by single, individual stellar photons (Draine & Li 2001) and will emit at the Si-C stretch, presumably at $11.3 \mu\text{m}$, which, because of the quantum-confinement effect, is expected to differ from the $11.3 \mu\text{m}$ absorption feature associated with the (crystalline) bulk phase of SiC. Like crystalline silicate nanoparticles, the $11.3 \mu\text{m}$ emission feature of SiC nanoparticles will probably be hidden by that of polycyclic aromatic hydrocarbon molecules (see Li & Draine 2001).

Admittedly, the average mass loss rates and total numbers for carbon stars in the Galaxy are not accurately known. The dust production rates of carbon stars depend on the star formation history and metallicity of the galaxy under consideration. The SiC mass fraction depends on the metallicity as well. Nanni et al. (2019) found that the SiC mass fraction could be up to 43% of the total dust mass produced by the carbon stars in the Large Magellanic Cloud and 11% for the Small Magellanic Cloud. However, these are upper limits reached by the dustiest carbon stars, and the spreads in the SiC mass fractions are large (see Figure 9 of Nanni et al. 2019). As a consequence, the injection rate of SiC dust into the ISM may be much smaller. In Groenewegen et al. (1998) where the spectral energy distribution fitting had been performed for carbon stars in the Galaxy, the SiC mass fractions are smaller than 10% for most (37/44) of their stars. Therefore, the nondetection of the $11.3 \mu\text{m}$ absorption feature of SiC dust could merely be due to a lower injection rate of carbon dust and/or a lower SiC mass fraction than that adopted here.

Alternatively, as argued by Draine (1990), interstellar dust is *not* stardust, i.e., the bulk of the solid material in interstellar grains actually condensed in the ISM rather than in stellar outflows. While carbon stars do eject an appreciable amount of SiC dust into the ISM, supernova shock waves destroy SiC dust (as well as silicate and carbon dust) at a

⁵ While Amari et al. (1994) found that $\sim 20\%$ of all the presolar SiC grains seen in the Murchison meteorite is in the fractions greater than $1 \mu\text{m}$ and only about 4% in the fraction less than $0.3 \mu\text{m}$, NanoSIMS measurements of the Murchison meteorite with a resolution of $\sim 50 \text{ nm}$ revealed that submicron-sized grains are much more abundant than their larger, micron-sized counterparts (see Hoppe et al. 2010).

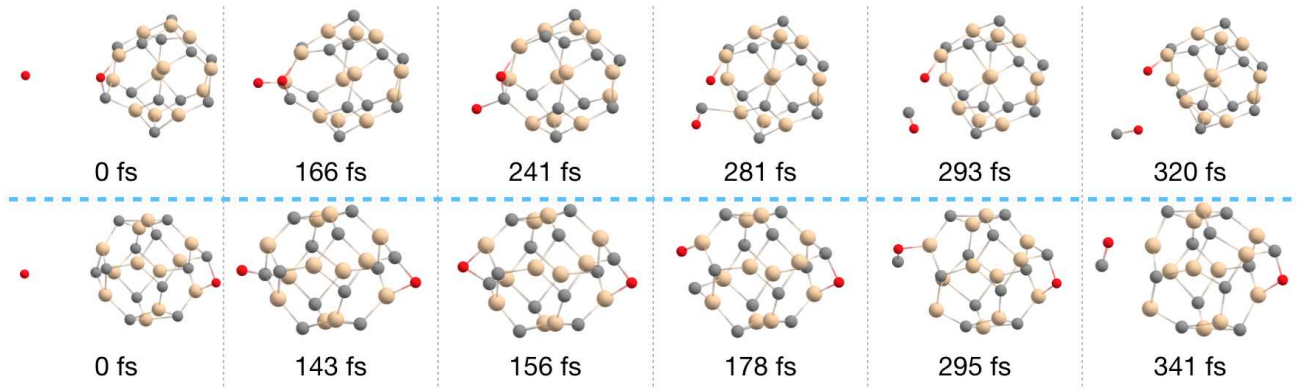


Figure 5. Snapshots from molecular dynamics simulations for collisions between an oxygen atom (red ball) and a $\text{Si}_{12}\text{C}_{12}\text{O}$ molecule from two opposite directions.

rate faster than its production (McKee 1989), while grain re-growth in the oxygen-rich ISM unlikely leads to SiC.

Finally, we note that the B3LYP hybrid functional employed here had been shown to outperform for SiC cluster systems (see Byrd et al. 2016). While the triangle isomer of Si_3C_3 and the spherical isomer $\text{Si}_{12}\text{C}_{12}$ adopted here correspond to their respective global minimum based on DFT calculations made at the M11/cc-pvTZ level of theory (Gobrecht et al. 2017), a different global minimum which is lower than the spherical isomer by $>0.4\text{ eV}$ was found for $\text{Si}_{12}\text{C}_{12}$ from calculations at the B3LYP/6-311++G(2d,p) level (Byrd et al. 2016). In view of this inaccuracy, we have also calculated the binding energies for the $\text{O} + \text{Si}_3\text{C}_3$ system and the $\text{O} + \text{Si}_{12}\text{C}_{12}$ system using the M11/cc-pvTZ level of theory applied by Byrd et al. (2016). It is found that the energy difference between M11/cc-pvTZ and B3LYP/6-311++G(2d,p) is at most 0.24 eV for $\text{O} + \text{Si}_3\text{C}_3$ and only $\sim 0.01\text{ eV}$ for $\text{O} + \text{Si}_{12}\text{C}_{12}$. Such energy differences will not affect the major results of this work.

5 CONCLUSION

We have utilized molecular dynamics simulations and performed DFT calculations to investigate the oxidation of SiC dust in the ISM. It is found that, although the reaction of an oxygen atom with a SiC molecule is exothermic and could cause CO-loss, the destruction rate of SiC dust through oxidation is considerably smaller than the currently believed stellar injection rate and therefore the nondetection of the $11.3\ \mu\text{m}$ absorption feature of SiC dust in the diffuse ISM cannot be explained by the destruction of SiC dust through oxidation, unless the currently believed SiC dust injection rate from carbon stars is overestimated and/or interstellar SiC dust is considerably smaller than submicron in size.

ACKNOWLEDGEMENTS

The calculations were performed on resources provided by the Swedish National Infrastructure for Computing (SNIC). We thank D. Gobrecht, M.A.T. Groenewegen, P.F. Miceli, A. Nanni, D.J. Singh, X.J. Yang and the anonymous referees

for very helpful suggestions. CYX is supported in part by the Talents Recruiting Program of Beijing Normal University and the NSFC Grant No.91952111. A.L. is supported in part by NSF AST-1816411 and NASA 80NSSC19K0572.

DATA AVAILABILITY

The data underlying this article will be shared on reasonable request to the corresponding authors.

REFERENCES

- Amari, S., Lewis, R. S., & Anders, E. 1994, *Geochim. Cosmochim. Acta*, 58, 459
- Becke, A. D. 1992, *J. Chem. Phys.*, 96, 2155
- Bernatowicz, T., Fraundorf, G., Ming, T., et al. 1987, *Nature*, 330, 728
- Byrd, J.N., Lutz, J.J., Jin, Y.F., et al. 2016, *J. Chem. Phys.*, 145, 024312
- Cristallo, S., Nanni, A., Cescutti, G., et al. 2020, *A&A*, 644, A8
- Dorfi, E., & Höfner, S. 1991, *A&A*, 248, 105
- Draine, B.T. 1990, in *ASP Conf. Ser. 12, The Evolution of the Interstellar Medium*, ed. L. Blitz (San Francisco: ASP), 193
- Draine, B.T. 2011, *Physics of the Interstellar and Intergalactic Medium* (Princeton, NJ: Princeton Univ. Press)
- Draine, B.T., & Li, A. 2001, *ApJ*, 551, 807
- Ervin, G. 1958, *J. Am. Ceram. Soc.*, 41, 347
- Friedemann, C. 1969, *Astron. Nachr.*, 291, 177
- Frisch, M. J., Trucks, G. W., Schlegel, H. B., et al. 2016, *Gaussian 16, Revision C. 01*, Gaussian, Inc., Wallingford CT
- Gehrz, R.D. 1989, in *IAU Symp. 135, Interstellar Dust*, ed. L. J. Allamandola & A. G. G. M. Tielens (Dordrecht: Kluwer), 445
- Gilman, R.C. 1969, *ApJ*, 155, L185
- Gobrecht, D., Cristallo, S., Piersanti, L., & Bromley, S. T. 2017, *ApJ*, 840, 117
- Grimme, S., Ehrlich, S., & Goerigk, L. 2011, *J. Comput. Chem.*, 32, 1456
- Groenewegen, M. A. T., Whitelock, P. A., Smith, C. H., et al. 1998, *MNRAS*, 293, 18
- Groenewegen, M. A. T., Sloan, G. C., Soszyński, I., et al. 2009, *A&A*, 506, 1277
- Helgaker, T., Uggerud, E., & Jensen, H.J.A. 1990, *Chem. Phys. Lett.*, 173, 145
- Hoppe, P., Leitner, J., Gröner, E. et al. 2010, *ApJ*, 719, 1370

- Kraemer, K. E., Sloan, G. C., Keller, L. D., et al. 2019, *ApJ*, 887, 82
- Larsson, B., Liseau, R., Pagani, L., et al. 2007, *A&A*, 466, 999
- Lee, C., Yang, W., & Parr, R. G. 1988, *Phys. Rev. B*, 37, 785
- Li, A. & Draine, B.T. 2001, *ApJ*, 550, L213
- McKee, C.F. 1989, in *IAU Symp. 135, Interstellar Dust*, ed. L. J. Allamandola & A. G. G. M. Tielens (Dordrecht: Kluwer), 431
- Meyer, D.M., Jura, M., & Cardelli, J.A. 1998, *ApJ*, 493, 222
- Mühhäuser, M., Froudakis, G., Zdetsis, A., & Peyerimhoff, S.D. 1993, *Chem. Phys. Lett.*, 204, 617
- Mutschke, H., Andersen, A. C., Clément, D., Henning, Th., & Peiter, G. 1999, *A&A*, 345, 187
- Nanni, A., Bressan, A., Marigo, P., et al. 2013, *MNRAS*, 434, 2390
- Nanni, A., Bressan, A., Marigo, P., et al. 2014, *MNRAS*, 438, 2328
- Nanni, A., Groenewegen, M. A. T., Aringer, B., et al. 2019, *MNRAS*, 487, 502
- Nanni, A., Cristallo, S., van Loon, J. T., et al. 2021, *Universe*, 7, 233
- Park, D.J., Jung, Y.I., Kim, H.G., Park, J.Y., & Koo, Y.H. 2014, *Corros. Sci.*, 88, 416
- Sloan, G. C., Kraemer, K. E., McDonald, I., et al. 2016, *ApJ*, 826, 44
- Speck, A. K., Barlow, M. J., & Skinner, C. J. 1997, *MNRAS*, 288, 431
- Treffers, R., & Cohen, M. 1974, *ApJ*, 188, 545
- Uggerud, E., & Helgaker, T. 1992, *J. Am. Chem. Soc.*, 114, 4265
- van Loon, J. T., Cioni, M.-R., Zijlstra, A. A., & Loup, C. 2005, *A&A*, 438, 273
- Ventura, P., di Criscienzo, M., Schneider, R., et al. 2012, *MNRAS*, 424, 2345
- Ventura, P., Dell'Agli, F., Schneider, R., et al. 2014, *MNRAS*, 439, 977
- Ventura, P., Karakas, A., Dell'Agli, F., García-Hernández, D.A., Guzman-Ramirez, L. 2018, *MNRAS*, 475, 2282
- Watkins, M. B., Shevlin, S. A., Sokol, A. A., et al. 2009, *Phys. Chem. Chem. Phys.*, 11, 3186
- Whittet, D.C.B., Duley, W.W., & Martin, P.G. 1990, *MNRAS*, 244, 427
- Wildt, R. 1933, *Zeitschr. für Astrophys.*, 6, 345
- Zhukovska, S., & Henning, Th. 2013, *A&A*, 555, A99

This paper has been typeset from a \TeX / \LaTeX file prepared by the author.